Gas-liquid phase separation in oppositely charged colloids: Stability and interfacial tension

Andrea Fortini,[a] Antti-Pekka Hynninen,[b] and Marjolein Dijkstra
Soft Condensed Matter, Utrecht University, Princetonplein 5, 3584CC Utrecht, The Netherlands

(Received 12 June 2006; accepted 14 July 2006; published online 1 September 2006)

We study the phase behavior and the interfacial tension of the screened Coulomb (Yukawa) restricted primitive model (YRPM) of oppositely charged hard spheres with diameter σ using Monte Carlo simulations. We determine the gas-liquid and gas-solid phase transitions using free energy calculations and grand-canonical Monte Carlo simulations for varying inverse Debye screening length κ. We find that the gas-liquid phase separation is stable for $\kappa\sigma \leqslant 4$, and that the critical temperature decreases upon increasing the screening of the interaction (decreasing the range of the interaction). In addition, we determine the gas-liquid interfacial tension using grand-canonical Monte Carlo simulations. The interfacial tension decreases upon increasing the range of the interaction. In particular, we find that simple scaling can be used to relate the interfacial tension of the YRPM to that of the restricted primitive model, where particles interact with bare Coulomb interactions. © *2006 American Institute of Physics*. [DOI: 10.1063/1.2335453]

I. INTRODUCTION

Coulombic interactions are important in a wide variety of physical systems such as electrolytes, molten salts, plasmas, colloidal suspensions, micelles, microemulsions, and liquid metals. The screened Coulomb (Yukawa) potential arises naturally for charged particles in the presence of a screening distribution of microions. The phase behavior of a pure system of hard spheres interacting with screened Coulomb potentials has been well studied and the phase diagram displays stable fluid, fcc, and bcc crystal phases.[1–4] In this paper, we study a binary fluid of oppositely charged particles using computer simulations. While the phase diagram of the restricted primitive model (RPM), consisting of a binary mixture of equally sized hard spheres carrying opposite charges of equal magnitude, and interacting with bare Coulombic interactions, has been widely studied,[5–12] there is little information available on the phase diagram of the Yukawa restricted primitive model (YRPM), where the hard spheres of diameter σ interact with screened Coulomb potentials $u_{ij} = \pm \epsilon\sigma \exp[-\kappa(r_{ij}-\sigma)]/r_{ij}$, with r_{ij} the distance between particles i and j, ϵ the contact value, and κ the Debye screening parameter (inverse of the Debye screening length). Recently, Hynninen *et al.*[13] determined the full phase diagram of the YRPM for a screening parameter $\kappa\sigma=6$. At high temperatures, the system behaves like a pure hard-sphere system, with a transition between a fluid and a substitutionally disordered fcc phase, where the opposite charges are distributed randomly on a fcc lattice. At lower temperatures, a dilute gas phase coexists with a high density CsCl solid phase, and the gas-liquid transition is metastable with respect to freezing. At high densities, various solid-solid transitions appear, e.g., a transition from CsCl to CuAu and from CuAu to the tetragonal phase. Overall the system exhibits a phase behavior in striking similarity with the RPM phase diagram,[7–10,13] which displays a fluid-disordered fcc transition at high temperatures, a stable gas-liquid transition at low temperatures, and a fluid-solid transition at higher densities. Since the RPM is the limit of the YRPM for $\kappa\sigma \to 0$, we expect a crossover from a metastable to a stable gas-liquid transition for $0 < \kappa\sigma < 6$.

The gas-liquid transition for a similar model with pair potential $u_{ij} = \epsilon \exp[-\kappa(r_{ij}-\sigma)]$ has been studied using computer simulations.[14–16] This interaction potential differs by a factor σ/r_{ij} from our model. The factor σ/r_{ij} is of the order of unity, and we expect the effect on the phase behavior to be small. This allows us to compare the results of Refs. 14–16 with the results of the YRPM. In particular, Caballero *et al.*[15] investigated the critical temperature as a function of the screening parameter. In a later paper,[16] the stability of the gas-liquid separation with respect to the gas-solid transition was estimated by computing the melting density of the CsCl structure. This technique overestimates the stability of the gas-liquid binodal, with respect to our free energy calculations. We will discuss the relationship between our results and those of Ref. 16 in more detail in Sec. IV.

An experimental realization of the YRPM is provided by charge-stabilized colloidal suspensions. Recently, it was shown experimentally that the charge on the colloids can be tuned in such a way that oppositely charged colloids can form large equilibrium ionic colloidal crystals.[13,17–19] Experiments, theory, and simulations based on screened Coulomb interactions are in good agreement. The system studied in Refs. 13 and 17 had a Debye screening parameter $\kappa\sigma \sim 7$, and a gas-liquid phase separation was not observed.

The critical temperature and structure of the YRPM has also been studied using integral equation theory,[20] but no information on the stability of the gas-liquid transition with respect to freezing has been given.

[a]Electronic mail: a.fortini@phys.uu.nl
[b]Present address: Department of Chemical Engineering, Princeton University, Princeton, NJ 08544.

The purpose of this paper is to determine the value of the screening parameter $\kappa\sigma$ at which the gas-liquid transition becomes stable for oppositely charged colloids. To this end, we perform Monte Carlo simulations to compute the Helmholtz free energies of the fluid and solid phases of the YRPM. We also study the dependence of the critical parameters and the gas-liquid interfacial tension on the interaction range. The critical parameters and the values of the interfacial tension are calculated using histogram reweighting methods and grand-canonical Monte Carlo simulations. The paper is organized as follows. In Sec. II, we describe the model, and we present the simulation methods in Sec. III. The results are discussed in Sec. IV and we end with some concluding remarks in Sec. V.

II. MODEL

We investigate the YRPM consisting of N spherical particles with a hard-core diameter σ in a volume V. Half of the spheres carry a positive charge and the other half a negative charge of the same magnitude. The pair interaction reads

$$\beta u(r_{ij}) = \begin{cases} \infty, & r_{ij} \leqslant \sigma \\ \pm \dfrac{\epsilon_Y}{k_B T} \dfrac{\exp[-\kappa(r_{ij}-\sigma)]}{r_{ij}/\sigma}, & \sigma < r_{ij} < r_{\mathrm{cut}} \\ 0, & \text{otherwise}, \end{cases} \quad (1)$$

where r_{ij} is the distance between spheres i and j, κ the screening parameter, $\beta \equiv 1/k_B T$ the inverse temperature with k_B the Boltzmann constant and T the temperature, and ϵ_Y the contact value of the potential. The cutoff value is $r_{\mathrm{cut}}=3.6\sigma$. The interaction is attractive for oppositely charged spheres, and repulsive for like-charged spheres. We define a reduced temperature $T_Y^*=k_B T/\epsilon_Y$ and measure particle density in terms of the packing fraction $\eta=(\pi\sigma^3/6)N/V$.

According to the Derjaguin-Landau-Verwey-Overbeek (DLVO) theory,[21,22] the effective pair potential between two charged spheres carrying the same number Z of elementary charges e suspended in a sea of salt ions with density ρ_s is given by Eq. (1) with a contact value

$$\frac{\epsilon_Y}{k_B T} = \frac{Z^2}{(1+k\sigma/2)^2} \frac{\lambda_B}{\sigma}. \quad (2)$$

The Debye screening parameter reads $\kappa=\sqrt{8\pi\lambda_B\rho_s}$, where $\lambda_B=e^2/\epsilon_s k_B T$ is the Bjerrum length and ϵ_s is the dielectric constant of the solvent. It must be noted that more recent theories on same charged colloidal spheres suspended in a sea of salt ions yield potentials of the form of Eq. (1), but with screening parameters that depend on the charged colloid concentration.[23–29] However, the exact functional form is yet unknown[30] and different theories predict varying functional forms. Furthermore, the DLVO theory was not originally derived for oppositely charged spheres, but it can be extended using the linear superposition approximation (LSA) to obtain the potential given by Eqs. (1) and (2).[31] The extended DLVO theory has been shown to give good agreement with Poisson-Boltzmann[32] and primitive model calculations[33] at small $\kappa\sigma$, justifying the use potential in Eq. (1) with the contact value given by Eq. (2). We will refer to the DLVO theory extended by the LSA simply as the DLVO theory. To facilitate the comparison between the results of the DLVO theory for different screening lengths κ, we define a reduced temperature $T_C^*=\sigma/Z^2\lambda_B$ that is independent of κ and equal to the the definition of the reduced temperature of the RPM.

III. SIMULATION METHODS

In order to determine the stable phase for a given state point, we compute the Helmholtz free energy as a function of η and T_Y^*. As the free energy cannot be measured directly in a Monte Carlo simulation, we use thermodynamic integration[34–36] to relate the free energy of the YRPM system to that of a reference system, whose free energy is known. In the thermodynamic integration of the fluid phase, we use the hard-sphere fluid as the reference state, whereas in the solid phase, the reference state is the Einstein crystal. We use a 10-point Gaussian quadrature for the numerical integrations and the ensemble averages are calculated from runs with 40 000 Monte Carlo (MC) cycles (attempts to displace each particle once), after first equilibrating the system during 20 000 MC cycles. Employing a common tangent construction on the fluid free energy density curves as a function of η, we find the points of tangency that correspond to the densities of the coexisting gas and liquid phase. A similar common tangent construction is used to determine the coexistence between the fluid and solid phases, and to check whether the gas-liquid separation is stable with respect to the fluid-solid phase coexistence. In addition, we perform a more detailed study of the gas-liquid binodal using methods based on histogram reweighting. To this end, we employ grand-canonical MC simulations with successive umbrella sampling[37] to overcome the free energy barrier between the liquid and gas phases. In the successive umbrella sampling method, the probability $P(N)|_{z_+,z_-}$ of having N particles at fugacity $z=z_+=z_-$ in a volume $V=L^3$ is obtained by sampling successively "windows" of particle numbers. In each window, the number of spheres N is allowed to fluctuate by one particle, i.e., between 0 and 1 in the first window, 1 and 2 in the second window, etc. We choose at random whether to make an attempt to insert or to remove a particle such that, on average, the system is charge neutral. The sampling of the probability ratio $P(N)/P(N+1)$ is done, in each window, until the difference between two successive samplings of the probability ratio is smaller than 10^{-3}. At phase coexistence, the (normalized) distribution function $P(N)|_z$ becomes bimodal, with two separate peaks of equal area for the liquid and gas phases. To determine phase coexistence we calculate the average number of particles,

$$\langle N \rangle = \int_0^\infty N P(N)|_z dN. \quad (3)$$

Subsequently, we use the histogram reweighting technique[38] to determine the fugacity z' for which the equal area rule

$$\int_0^{\langle N \rangle} P(N)|_{z'} dN = \int_{\langle N \rangle}^\infty P(N)|_{z'} dN, \quad (4)$$

which is the condition for phase coexistence, is satisfied.

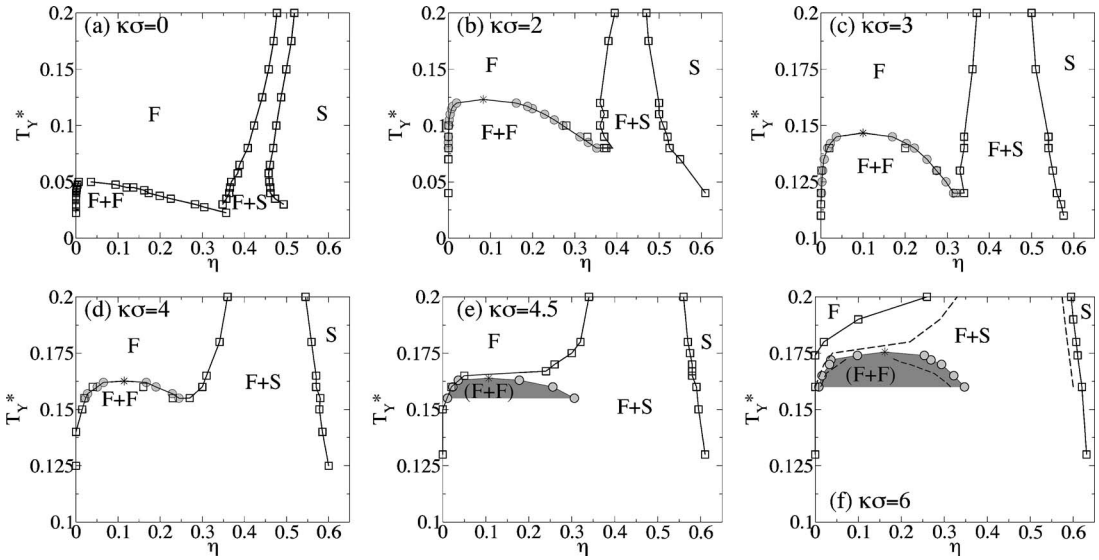

FIG. 1. Phase diagrams of the YRPM in the reduced temperature T_Y^*: packing fraction η representation for varying Debye screening parameter (a) $\kappa\sigma=0$ from Refs. 5, 6, and 10; (b) $\kappa\sigma=2$; (c) $\kappa\sigma=3$; (d) $\kappa\sigma=4$; (e) $\kappa\sigma=4.5$; (f) $\kappa\sigma=6$. The squares are the results from the free energy calculations and the circles are the results from the grand-canonical Monte Carlo simulations. F and S denote the stable fluid and solid (CsCl) phases. $F+S$ and $F+F$ denote, respectively, stable fluid-solid and (meta) stable gas-liquid coexistence region (the shaded regions are metastable). The dashed line in (f) indicates the results of the model used by Caballero and Puertas (Ref. 16). The lines are a guide to the eye. Tie lines (not shown) are horizontal.

The gas-liquid interfacial tension γ_{lg} for a finite system with volume $V=L^3$ is obtained from $P(N)|_{z'}$ at coexistence,

$$\beta\gamma_{lg,L}=\frac{1}{2L^2}\left[\ln\left(\frac{P(N_{\max}^g)+P(N_{\max}^l)}{2}\right)-\ln(P(N_{\min}))\right], \tag{5}$$

where $P(N_{\max}^g)$ and $P(N_{\max}^l)$ are the maxima of the gas and liquid peaks, respectively, and $P(N_{\min})$ is the minimum between the two peaks. We determine the bulk interfacial tension γ_{lg} by performing simulations for a range of system sizes and by extrapolating the results to the infinite system size using the relation[39–41]

$$\beta\gamma_{lg,L}=\beta\gamma_{lg}-\frac{x\ln L}{2L^2}-\frac{\ln A}{2L^2}, \tag{6}$$

where A and x are generally unknown. The finite size scaling is performed using the simulation results for box lengths $L/\sigma=8$, 10, 12, and 14.

The critical temperature T_{cr} and critical packing fraction η_{cr} are determined by fitting the scaling law

$$\eta_l-\eta_g=f_1(T_{cr}-T)^{0.32}, \tag{7}$$

and the law of rectilinear diameters

$$\frac{\eta_l+\eta_g}{2}=\eta_{cr}+f_2(T_{cr}-T), \tag{8}$$

to the simulation results for the gas (η_g) and liquid (η_l) packing fractions, where f_1 and f_2 are fitting parameters.

IV. RESULTS

We compute the phase diagram using thermodynamic integration and grand-canonical Monte Carlo simulations for screening parameters $\kappa\sigma=2$, 3, 4, 4.5, and 6. In Fig. 1, we show the resulting phase diagrams in the (η, T_Y^*) plane, together with the $\kappa\sigma=0$ phase diagram from Refs. 10 (fluid-solid), 5, and 6 (gas-liquid). The squares denote the results from the free energy calculations, and the circles represent the gas-liquid binodal obtained from the grand-canonical MC simulations. We find good agreement between both results. The shaded areas in Figs. 1(e) and 1(f) represent the metastable gas-liquid regions for screening parameters $\kappa\sigma=6$ and 4.5. For smaller screening parameters, $\kappa\sigma=4$, 3, and 2, the gas-liquid transition is stable, and the phase diagram resembles that of a simple fluid. At sufficiently low temperatures, a gas-liquid phase separation (metastable for screening parameters $\kappa\sigma=6$ and 4.5) appears at low densities and a fluid-solid transition at high density. At the triple point, the gas, liquid, and the solid phases are in coexistence, while at the critical point, the gas and the liquid phases have the same density. At temperatures below the triple point, a dilute gas coexists with a high density solid, and at temperatures higher than the critical temperature, a fluid coexists with a solid phase. Figure 1 shows that the region of stable liquid phase increases upon increasing the range of the interaction, i.e., decreasing $\kappa\sigma$. For simple fluids with short-range attractive

TABLE I. Critical temperatures $T_{Y,cr}^*$ and packing fractions η_{cr} for the YRPM for different values of the Debye screening parameter $\kappa\sigma$. The GMSA theory data is from Ref. 20.

	Simulation		GMSA theory	
$\kappa\sigma$	$T_{Y,cr}^*$	η_{cr}	$T_{Y,cr}^*$	η_{cr}
6	0.1755(5)	0.162(8)	0.160 53	0.150 40
4	0.1626(1)	0.114(3)	0.164 98	0.119 61
3	0.1467(1)	0.100(1)	0.162 40	0.095 66
2	0.1232(8)	0.083(1)		
0	0.0490(3)[a]	0.037(3)	0.078 58	0.014 48

[a]Data from Orkoulas and Panagiotopoulos (Ref. 49).

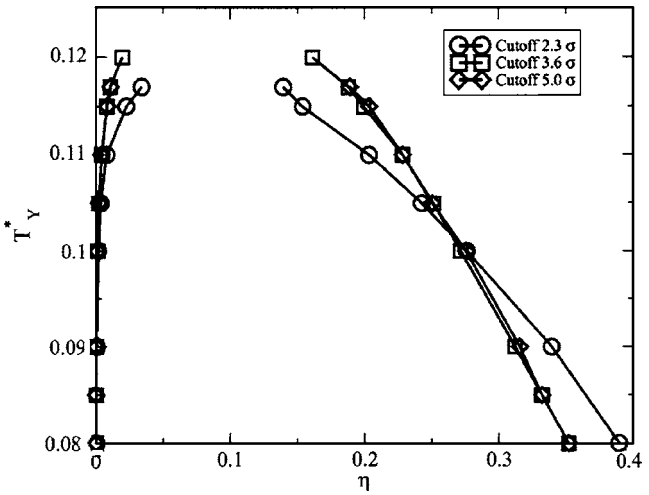

FIG. 2. Binodals of the YRPM for screening parameter $\kappa\sigma=2$, and cutoff values $r_{cut}/\sigma=2.3$, 3.6, and 5 in the (η, T_Y^*) representation. Statistical errors are of the order of the symbol size. The lines are a guide to the eye.

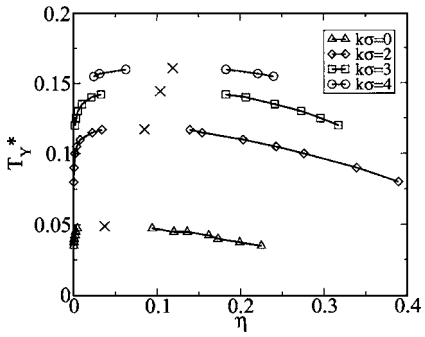

FIG. 3. Binodals and the critical points of the YRPM for screening parameters $\kappa\sigma=0$, 2, 3, and 4, in the (η, T_Y^*) representation. Crosses denote the location of the critical points. The binodal for $\kappa\sigma=0$ (RPM) is taken from Ref. 5 and the critical point from Ref. 49. The lines are a guide to the eye.

Yukawa interactions, square-well attractions, and depletion attractions, the relationship between the range of the attractive interactions and the stability of the gas-liquid transition has been well-studied by computer simulations, density functional calculations, and integral equation theories.[42–48] These studies show that the minimum range of attractions required for a stable gas-liquid transition is about one sixth of the range of the repulsions.

Our results show that the gas-liquid coexistence is stable for $\kappa\sigma \leqslant 4$, and therefore contradict the findings of Ref. 16, where an estimate $\kappa\sigma \leqslant 25$ was given. In this comparison we have to keep in mind that the pair potential used in Ref. 16 did not include the factor $1/r$, which we include. To study the effect of this factor, we repeated our free energy calculations using the pair potential of Ref. 16 for screening length $\kappa\sigma=6$. The results for this model are presented in Fig. 1(f) with a dashed line. We find that there is no qualitative difference between the two models; both predict a metastable gas-liquid transition for screening length $\kappa\sigma=6$. In Ref. 16, the stability of the gas-liquid transition was determined from the crossover between the freezing line and the liquid branch of the gas-liquid binodal. The crossover point was recognized as the gas-liquid-solid triple point. When the triple point was at a lower temperature than the critical point, the gas-liquid phase separation was considered stable. Since the CsCl structure melts in the middle of the broad gas-solid coexistence, the criteria used in Ref. 16 would indicate a stable gas-liquid separation, whereas our free energy calculations show that it is, in fact, metastable. We argue that the computation of the melting line cannot be used to determine the stability of gas-liquid transition with respect to a broad gas-solid coexistence region.

It is interesting to note that previous simulation studies of a one-component hard-core attractive Yukawa fluid predict a stable gas-liquid transition for $\kappa\sigma=3.9$, while it is metastable for $\kappa\sigma=7$,[42,48] which compares well with our results.

Table I summarizes the critical temperatures $T_{Y,cr}^*$ and critical packing fractions η_{cr} as found from our simulations and from the generalized mean spherical approximation (GMSA) theory[20] for different values of $\kappa\sigma$.

In Fig. 2, we analyze the effect of the cutoff value of Eq. (1) on the liquid-gas binodal. Huge deviations are expected as the interaction becomes longer ranged. We used three different cutoff values $r_{cut}/\sigma=2.3$, 3.6, and 5 for the calculation of the liquid-gas binodal for our longest range interaction $(\kappa\sigma=2)$. The binodals for cutoff values $r_{cut}/\sigma=3.6$, and 5 are equivalent within the statistical accuracy, thereby justifying the choice of a cutoff value $r_{cut}/\sigma=3.6$ in all subsequent calculations.

Figure 3 shows the (stable) gas-liquid binodals for $\kappa\sigma=2$, 3, and 4, in the (η, T_Y^*) representation. Table I and Fig. 3 show that, for $0 \leqslant \kappa\sigma \leqslant 6$, the reduced critical temperature $T_{Y,cr}^*$ and the critical packing fraction η_{cr} decrease for increasing range of the interaction, i.e., decreasing $\kappa\sigma$, in agreement with the findings of Caballero *et al.*[15] The nonmonotonic behavior of the critical temperature as a function of $\kappa\sigma$ that was reported in Ref. 15 for screening parameters $\kappa\sigma > 10$ is in the region where we claim the gas-liquid phase

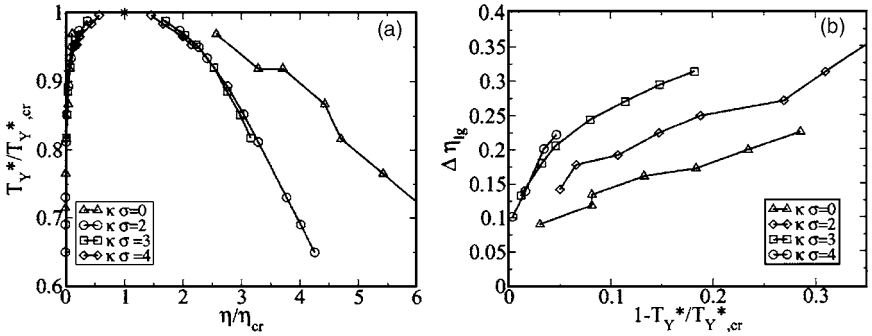

FIG. 4. (a) Binodals of the YRPM and the RPM in the corresponding state representation for Debye screening parameters $\kappa\sigma=2$, 3, and 4. The reduced temperature T_Y^* is scaled with the critical temperature $T_{Y,cr}^*$ and the packing fraction η is scaled with the critical packing fraction η_{cr}. The binodal for $\kappa\sigma=0$ (RPM) is from Ref. 5 and the critical point from Ref. 49. (b) The difference in coexisting packing fractions $\Delta\eta_{lg}=\eta_l-\eta_g$ is plotted against $1-T_Y^*/T_{Y,cr}^*$.

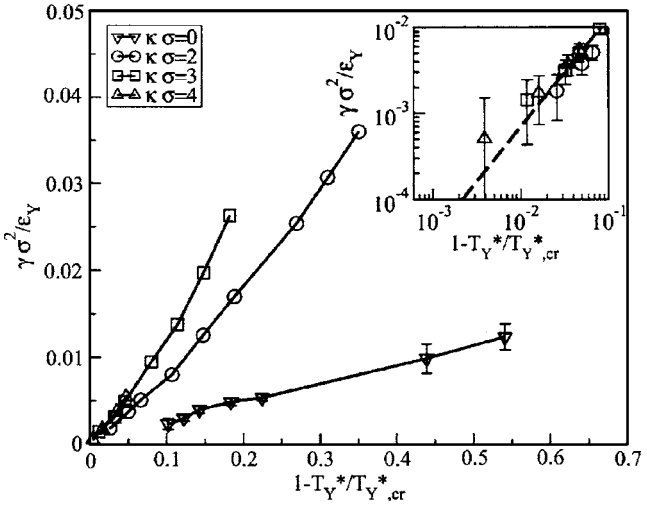

FIG. 5. Dimensionless gas-liquid interfacial tension $\gamma_{lg}\sigma^2/\epsilon_Y$ as a function of $1-T^*_{Y,cr}/T^*_Y$. The data for $\kappa\sigma=0$ is from Ref. 50. Inset: log-log plot of the dimensionless interfacial tension in the vicinity of the critical point. The dashed line is the theoretical prediction (Refs. 51 and 52) $\gamma\sim(T^*_{Y,cr}-T^*_Y)^{1.26}$.

separation to be metastable. As can be seen from Table I, the GMSA theory predicts a nonmonotonic behavior of the critical temperature as a function of $\kappa\sigma$. Comparing the theoretical results with our simulations, we observe that the GMSA theory overestimates the critical temperature for $\kappa\sigma<6$ and underestimates it at $\kappa\sigma=6$. On the other hand, the GMSA theory underestimates the critical packing fraction η_{cr} at $\kappa\sigma=0$, but agrees reasonably well with our simulation results for $\kappa\sigma\geqslant 3$.

Figure 4(a) shows the binodals of the YRPM and the RPM in the corresponding state representation, where the reduced temperature T^*_Y is scaled with the critical temperature $T^*_{Y,cr}$, and the packing fraction η is scaled with the critical packing fraction η_{cr}. We see that the binodals do not collapse on a single master curve, but instead, the RPM binodal (where $\kappa\sigma=0$) differs considerably from the YRPM binodals (where $\kappa\sigma=2$, 3, and 4). This finding is in agreement with the prediction of the GMSA theory.[20] In Fig. 4(b), we plot the width of the gas-liquid separation, $\Delta\eta_{lg}=\eta_l-\eta_g$, as a function of $1-T^*_Y/T^*_{Y,cr}$. We see that for a fixed $1-T^*_Y/T^*_{Y,cr}$, the width of the gas-liquid separation decreases with increasing range of the interaction, resulting in a smaller density gap between the coexisting liquid and gas phase for longer-ranged interactions.

Figure 5 shows the gas-liquid interfacial tension, scaled with the contact value energy ϵ_Y, for different values of the screening parameter $\kappa\sigma$. For comparison, we also show the interfacial tension of the RPM from Ref. 50. As can be seen from Fig. 5, the value of the dimensionless interfacial tension increases with increasing $\kappa\sigma$. This can be understood on the basis of Fig. 4(b), which shows that, with increasing $\kappa\sigma$, the density gap of the coexistence region increases, meaning that the interfacial tension increases. The inset of Fig. 5 shows a log-log plot of $\gamma_{lg}\sigma^2/\epsilon_Y$ vs $1-T^*_Y/T^*_{Y,cr}$ in the vicinity of the critical point, which can be used to extract an estimate for the critical exponent of the correlation length ν. We found $2\nu\simeq 1.1$ for all screening parameters $\kappa\sigma$, by performing a linear fit on the data, which differs from the Ising model result $2\nu=1.32$,[39] and from the accepted value of $2\nu=1.26$.[51,52] The value of the correlation length is very sensitive to the extrapolated surface tension to infinite system sizes. In order to improve the statistical accuracy of the simulations, larger system sizes, as well as longer runs are needed, especially close to the critical point. Nevertheless, our results are compatible within the simulation error, with the theoretical prediction of the correlation length (dashed line in the inset of Fig. 5).

We now interpret our results in view of the DLVO theory. In the DLVO theory, the contact value ϵ_Y, and hence the reduced temperature $T^*_Y=k_BT/\epsilon_Y$, depend on the salt concentration ρ_s through the screening parameter $\kappa\sigma$; see Eq. (2). In Fig. 6(a), we plot the gas-liquid binodals and critical points for $\kappa\sigma=0$, 2, 3, and 4, using the reduced temperature $T^*_C=\sigma/Z^2\lambda_B$ that does not depend on $\kappa\sigma$. As can be seen from Fig. 6(a), the reduced critical temperature $T^*_{C,cr}$ decreases with increasing $\kappa\sigma$, or salt concentration. This means that, at a fixed T^*_C and at a state point inside the gas-liquid coexistence region, adding salt decreases the density difference between the gas and the liquid phases, until, at the critical salt concentration, the density difference disappears. This finding could be confirmed by performing simulations with explicit coions and counterions,[30,53] and could be used to experimentally test the validity of the DLVO theory for oppositely charged colloids. Figure 6(b) shows the interfacial tension scaled with the contact value $\epsilon_C=Z^2k_BT\lambda_B/\sigma$, and as can be seen, the interfacial tensions for different $\kappa\sigma$ collapse to a single line. This suggests that the interfacial tension is determined solely by the contact value and not by the range of the interaction.

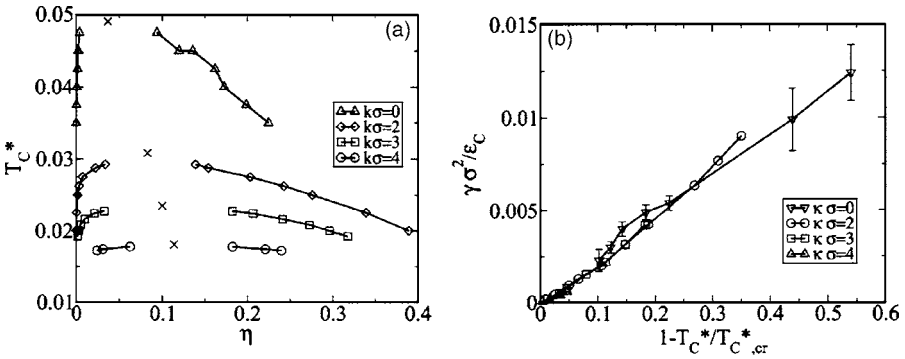

FIG. 6. (a) Binodals of the YRPM, for Debye screening parameters $\kappa\sigma=0$, 2, 3, and 4, in the reduced temperature T^*_C and the packing fraction η representation. The binodal for $\kappa\sigma=0$ (RPM) is from Ref. 5 and the critical point from Ref. 49. (b) Dimensionless gas-liquid interfacial tension $\gamma_{lg}\sigma^2/\epsilon_C$ as a function of $1-T^*_Y/T^*_{Y,cr}$. Remember that $T^*_C/T^*_{C,cr}=T^*_Y/T^*_{Y,cr}$. The data for $\kappa\sigma=0$ is from Ref. 50.

V. CONCLUSIONS

We have used a combination of MC free energy calculations and grand-canonical MC simulations to determine the stability and the interfacial tension of the gas-liquid phase separation in a binary mixture of oppositely charged hard spheres, which interact via screened-Coulomb (Yukawa) potentials. We find that the gas-liquid coexistence is stable with respect to gas-solid coexistence for values of the screening parameter $\kappa\sigma \leqslant 4$. This value is similar to what is found for the single component attractive Yukawa model,[48] where the gas-liquid transition is stable at $\kappa\sigma=4$ and metastable at $\kappa\sigma=7$.

We have studied the dependence of the critical temperature as a function of the range of the Yukawa interaction. If the contact value of the interaction potential does not depend on the screening length, it is possible to define a reduced critical temperature simply as the inverse of the Yukawa contact value. With this definition, the reduced critical temperature decreases upon increasing the range of the interaction, which is in agreement with Ref. 15.

We have related the YRPM to the DLVO theory, which was recently used to explain experimental results on oppositely charged colloids.[13,17,19,54] The DLVO theory predicts a contact value that depends on the screening length. Thus, in order to facilitate the comparison between the results for different screening lengths, we define a temperature scale that is independent of the screening length. The natural choice is the reduced temperature of the RPM, which is the limit of zero screening length of the DLVO theory. With this definition, the reduced critical temperature decreases upon increasing the range of the interaction. This means that upon adding salt to a system at fixed temperature and at a state point in the gas-liquid coexistence region, the density difference between the gas and liquid phases decreases, and finally disappears at the critical salt concentration. This prediction could be tested by computer simulations with explicit coions and counterions,[30,53] and could be used to study experimentally the validity of the DLVO theory for oppositely charged colloids.

Finally, we have studied the gas-liquid interfacial tension using histogram reweighting methods. We find that the dimensionless tension decreases for decreasing screening parameter. Upon scaling the interfacial tension with the contact value of the Coulomb interaction, we observed a collapse of the interfacial tensions onto a single curve. This means that for state points at coexistence and at the same scaled temperature $T_C^*/T_{C,\mathrm{cr}}^*$, the interfacial tension is determined solely by the contact value and not by the range of the interaction. There might be a possible connection with the well known similarities between the structures of the RPM and of the YRPM. Larsen and Rogde[55] noted that their Monte Carlo results for the radial distribution functions of the YRPM were similar to those obtained for the RPM at different state points. The structurally equivalent states were further investigated by Copestake and Evans[56] and by de Carvalho and Evans.[20] This correspondence is due to the screening of charges in the RPM, which in turn is due to charge ordering.[20,55,56] Consequently, the potential of mean force between two ions decays more rapidly than the bare Coulomb potential. For certain state points the potentials of mean force will be similar for the YRPM and the RPM. Preliminary results suggest that a similar explanation holds for the state points with similar interfacial tensions. Further investigation is in progress.

ACKNOWLEDGMENTS

We thank A. Cuetos and E. Sanz for many useful and inspiring discussions. We thank Athanassios Z. Panagiotopoulos for critical reading of the manuscript. This work is part of the research program of the Stichting voor Fundamenteel Onderzoek der Materie (FOM), that is financially supported by the Nederlandse Organisatie voor Wetenschappelijk Onderzoek (NWO). We thank the Dutch National Computer Facilities foundation for granting access to the LISA supercomputer.

[1] M. O. Robbins, K. Kremer, and S. Grest, J. Chem. Phys. **88**, 3286 (1988).
[2] E. J. Meijer and F. E. Azhar, J. Chem. Phys. **106**, 4678 (1997).
[3] F. E. Azhar, M. Baus, J. P. Ryckaert, and E. J. Meijer, J. Chem. Phys. **112**, 5121 (2000).
[4] A. P. Hynninen and M. Dijkstra, Phys. Rev. E **68**, 021407 (2003).
[5] G. Orkoulas and A. Z. Panagiotopoulos, J. Chem. Phys. **101**, 1452 (1994).
[6] C. Vega, F. Bresme, and J. L. Abascal, Phys. Rev. E **54**, 2746 (1996).
[7] B. Smit, K. Esselink, and D. Frenkel, Mol. Phys. **87**, 159 (1996).
[8] F. Bresme, C. Vega, and J. L. F. Abascal, Phys. Rev. Lett. **85**, 3217 (2000).
[9] J. L. F. Abascal, C. Vega, C. McBride, and F. Bresme, Phys. Rev. E **68**, 052501 (2003).
[10] C. Vega, J. L. F. Abascal, and C. McBride, J. Chem. Phys. **119**, 964 (2003).
[11] Y. V. Kalyuzhnyi, G. Kahl, and P. T. Cummings, J. Chem. Phys. **123**, 124501 (2005).
[12] M. E. Fisher, J.-N. Aqua, and S. Banerjee, Phys. Rev. Lett. **95**, 135701 (2005).
[13] A.-P. Hynninen, M. E. Leunissen, A. van Blaaderen, and M. Dijkstra, Phys. Rev. Lett. **96**, 018303 (2006).
[14] J. B. Caballero, A. M. Puertas, A. Fernández-Barbero, and F. J. de las Nieves, J. Chem. Phys. **121**, 2428 (2004).
[15] J. B. Caballero, A. M. Puertas, A. Fernández-Barbero, F. J. de las Nieves, J. Romero-Enrique, and L. Rull, J. Chem. Phys. **124**, 054909 (2006).
[16] J. B. Caballero and A. Puertas, e-print cond-mat/0511666.
[17] M. E. Leunissen, C. G. Christova, A.-P. Hynninen, C. P. Royall, A. I. Campbell, A. Imhof, M. Dijkstra, R. van Roij, and A. van Blaaderen, Nature (London) **437**, 235 (2005).
[18] P. Bartlett and A. I. Campbell, Phys. Rev. Lett. **95**, 128302 (2005).
[19] A.-P. Hynninen, C. G. Christova, R. van Roij, A. van Blaaderen, and M. Dijkstra, Phys. Rev. Lett. **96**, 138308 (2006).
[20] R. J. F. L. de Carvalho and R. Evans, Mol. Phys. **92**, 211 (1997).
[21] B. Derjaguin and L. Landau, Acta Physicochim. URSS **14**, 633 (1941).
[22] J. W. Verwey and J. T. G. Overbeek, *Theory of the Stability of Lyotropic Colloids* (Elsevier, Amsterdam, 1948).
[23] H. Graf and H. Löwen, Phys. Rev. E **57**, 5744 (1998).
[24] M. Dijkstra and R. van Roij, J. Phys.: Condens. Matter **10**, 1219 (1998).
[25] R. van Roij, M. Dijkstra, and J.-P. Hansen, Phys. Rev. E **59**, 2010 (1999).
[26] A. R. Denton, Phys. Rev. E **62**, 3855 (2000).
[27] P. B. Warren, J. Chem. Phys. **112**, 4683 (2000).
[28] L. Belloni, J. Phys.: Condens. Matter **12**, R549 (2000).
[29] B. Zoetekouw and R. van Roij, Phys. Rev. E **73**, 021403 (2006).
[30] A.-P. Hynninen and M. Dijkstra, J. Chem. Phys. **123**, 244902 (2005).
[31] G. M. Bell, S. Levine, and L. N. McCartney, J. Colloid Interface Sci. **33**, 335 (1970).
[32] G. R. Maskaly, Ph.D. thesis, Massachusetts Institute of Technology, 2005.
[33] A.-P. Hynninen, Ph.D. thesis, Utrecht University, 2005.
[34] D. Frenkel and B. Smit, *Understanding Molecular Simulation*, Computa-

tional Science Series Vol. 1, 2nd ed. (Academic, New York, 2002).
[35] D. Frenkel and A. J. C. Ladd, J. Chem. Phys. **81**, 3188 (1984).
[36] J. M. Polson, E. Trizac, S. Pronk, and D. Frenkel, J. Chem. Phys. **112**, 5339 (2000).
[37] P. Virnau and M. Müller, J. Chem. Phys. **120**, 10925 (2004).
[38] A. M. Ferrenberg and R. H. Swendsen, Phys. Rev. Lett. **61**, 2635 (1988).
[39] K. Binder, Phys. Rev. A **25**, 1699 (1982).
[40] J. J. Potoff and A. Z. Panagiotopoulos, J. Chem. Phys. **112**, 6411 (2000).
[41] R. L. C. Vink, J. Horbach, and K. Binder, Phys. Rev. E **71**, 011401 (2005).
[42] M. H. J. Hagen and D. Frenkel, J. Chem. Phys. **101**, 4093 (1994).
[43] P. Bolhuis, M. H. J. Hagen, and D. Frenkel, Phys. Rev. E **50**, 4880 (1994).
[44] C. F. Tejero, A. Daanoun, H. N. W. Lekkerkerker, and M. Baus, Phys. Rev. Lett. **73**, 752 (1994).
[45] C. F. Tejero, A. Daanoun, H. N. W. Lekkerkerker, and M. Baus, Phys. Rev. E **51**, 558 (1995).
[46] A. Daanoun, C. F. Tejero, and M. Baus, Phys. Rev. E **50**, 2913 (1994).
[47] C. Caccamo, G. Pellicane, D. Costa, D. Pini, and G. Stell, Phys. Rev. E **60**, 5533 (1999).
[48] M. Dijkstra, Phys. Rev. E **66**, 021402 (2002).
[49] G. Orkoulas and A. Z. Panagiotopoulos, J. Chem. Phys. **110**, 1581 (1999).
[50] M. González-Melchor, J. Alejandre, and F. Bresme, Phys. Rev. Lett. **90**, 135506 (2003).
[51] J. H. Chen, M. E. Fisher, and B. G. Nickel, Phys. Rev. Lett. **48**, 630 (1982).
[52] A. M. Ferrenberg and R. H. Swendsen, Phys. Rev. B **44**, 5081 (1991).
[53] A.-P. Hynninen, M. Dijkstra, and A. Z. Panagiotopoulos, J. Chem. Phys. **123**, 084903 (2005).
[54] G. R. Maskaly, R. E. Garcia, W. C. Carter, and Y.-M. Chiang, Phys. Rev. E **73**, 011402 (2006).
[55] B. Larsen and S. A. Rogde, J. Chem. Phys. **72**, 2578 (1980).
[56] A. P. Copestake and R. Evans, J. Phys. C **15**, 4961 (1982).